PROCEEDINGS OF SCIENCE

H.E.S.S. follow-up observation of GRB221009A

Jean Damascene Mbarubucyeye,[1,*] **Halim Ashkar,**[2] **Sylivia Zhu ,**[1] **Brian Reville**[3] **and Fabian Schüssler**[4] on behalf of the **H.E.S.S. Collaboration**
(a complete list of authors can be found at the end of the proceedings)

[1] *Deutsches Elektronen-Synchrotron (DESY), Platanenallee 6, 15738 Zeuthen, Germany*

[2] *Laboratoire Leprince-Ringuet, École Polytechnique, CNRS, Institut Polytechnique de Paris, F-91128 Palaiseau, France*

[3] *Max-Planck-Institut für Kernphysik, P.O. Box 103980, D 69029 Heidelberg, Germany*

[4] *IRFU, CEA, Université Paris-Saclay, F-91191 Gif-sur-Yvette, France*

E-mail: jean.mbarubucyeye@desy.de

GRB 221009A is the brightest gamma-ray burst ever detected. To probe the very-high-energy (VHE, >100 GeV) emission, the High Energy Stereoscopic System (H.E.S.S.) began observations 53 hours after the triggering event, when the brightness of the moonlight no longer precluded observations. No significant VHE emission from the gamma-ray burst is detected in an analysis of the obtained H.E.S.S. data. Differential and integral upper limits are computed using data from the third, fourth, and ninth nights after the initial detection of the GRB. The constraints derived from the H.E.S.S. observations complement the available multi-wavelength data. For example, the afterglow of GRB 221009A presents a novel opportunity to explore extreme Klein-Nishina effects, for which upper limits in the VHE band are valuable. We will present and discuss the results of the analysis and highlight the important role of IACTs in following up on such powerful events.

The 38th International Cosmic Ray Conference (ICRC2023)
26 July – 3 August, 2023
Nagoya, Japan

*Speaker

PoS(ICRC2023)705

1. Introduction

Gamma-Ray Bursts (GRBs) are some of the brightest X-ray and gamma-ray flashes and the most violent phenomena known in the universe to date. They release up to 10^{55} ergs of isotropic equivalent energy within typically a few seconds. They are seen as short intense pulsed periods of gamma-ray emission in the sub-MeV energy range lasting from 0.1 s up to a few hundred seconds. Such short-time intense emission phase is called the *prompt phase* of the GRB and is followed by the so-called *afterglow* phase which is the slowly fading emission that can be detectable over a large part of the electromagnetic spectrum for days or months. The two phases are explained in the widely accepted relativistic shock model known as *fireball-model* [1] and references therein. Particle acceleration occurs at multiple stages throughout the evolution of this model. It posits that when a new compact object forms, an extremely fast-moving jet, known as an ultra-relativistic jet, is generated by the compact object acting as the central engine. This engine emits plasma shells with varying Lorentz factors $\Gamma(t)$ that eventually collide with each other. Each collision between two shells results in shock acceleration, leading to the production of gamma-rays spanning a wide energy range from keV to potentially TeV. Eventually, the shells (along with the jet) encounter the unshocked interstellar medium, marking the beginning of the afterglow phase, where shock acceleration can occur once again. The ability of gamma-radiation generated during different stages of this phenomenon to escape from the object heavily depends on the density of the photon field. If the density is too high, gamma-gamma absorption occurs, causing a cascading effect that reduces the initial energy of the photons. Additionally, the highest energy photons can be absorbed through interactions with the Extragalactic Background Light (EBL) if the distance between the object and the observer is significant.

The prompt emission duration exhibits a bimodal distribution, suggesting the presence of two distinct classes known as Long GRBs and short GRBs. Long GRBs are thought to arise from the demise of rapidly rotating massive stars, where the star's core collapses [2], and a portion of the released energy is channeled into an intense blast wave that rips through the remnants of the star at near the speed of light. The origin of short GRBs has not been thoroughly understood, but there are indications suggesting that they may result from the mergers of compact objects, such as binary neutron stars [3]. The only existing and extensively examined evidence for short GRBs was the detection of GW 170817, which coincided with GRB 170817, followed by a Kilonova [4, 5].

The study of relativistic shocks in the physics of GRB afterglows presents a significant opportunity. The process of synchrotron emission, responsible for producing X-ray emissions, has been extensively researched and well understood. However, there is still ongoing debate surrounding the specificities of emission at higher energy levels, particularly in the very-high energy (VHE) gamma-ray (> 100 GeV) range. In recent years, several GRBs have been detected emitting VHE gamma rays. This VHE component is typically linked to the inverse Compton scattering of ambient or synchrotron photons, with the latter referred to as the synchrotron self-Compton (SSC) scenario. However, in the case of GRB 190829A [6], discrepancies between observations and the commonly used single-zone (uniform magnetic field) SSC explanation have been observed. To gain further insights into this unresolved matter, additional observations, particularly in the VHE gamma-ray range, are necessary.

The discovery of TeV gamma-ray emissions from Long GRBs in 2019 [6, 7] made the hint of

detection more plausible. Recently, the brightest burst since the beginning of human civilization was detected, prompting subsequent observations using multi-wavelength instruments. This burst is *GRB 221009A*, which is the subject of this contribution.

A substantial portion of this contribution has been published in [8].

2. GRB 221009A

GRB 221009A, known as The BOAT (Brightest GRB of All Time), was initially triggered by the Fermi Gamma-Ray Burst Monitor (GBM) on 2022-10-09 at 13:16:59 UTC, denoted as T_0 from here on. The prompt emission light curve initially consisted of a long pulse phase lasting nearly T_0+10 seconds. This was followed by an exceptionally bright multi-peak phase occurring between T_0+180 seconds and T0+280 seconds, at the very least. The T_{90}, measured by Fermi-GBM in the 10-1000 keV range, was determined to be 327 seconds [9]. Approximately one hour after T_0, the Fermi Large Area Telescope (LAT) also reported the GRB [10]. The GRB also triggered the Neil Gehrels Swift Observatory once it became visible to the Swift Burst Alert Telescope, an hour later [11].

The fluence of GRB 221009A was measured to be (0.21 ± 0.02) erg cm^{-2} and (0.19 erg cm^{-2}) in the 1-10000 keV bands, respectively [12] and references therein). The redshift of this GRB is estimated to be $z = 0.151$ based on optical observations conducted with the ESO X-shooter/Very Large Telescope (VLT) [13, 14]. A significant isotropic equivalent energy $E_{\rm iso}$ in the 1-10000 keV range was estimated as $(1.01 \pm 0.007) \times 10^{55}$ erg from the redshift and the fluence measured by Fermi-GBM [15, 16].

Optical measurements were conducted using multiple instruments. The afterglow of GRB 221009A was detected by the ESO VLT through observations carried out with the X-shooter spectrograph on one of the telescopes (UT3), starting at T_0 + 11.55 hours. X-ray and optical observations persisted until the source entered Sun-block, revealing a characteristic decay pattern of a GRB afterglow. Furthermore, the optical data provided indications of emission originating from an associated supernova [17]. The GRB has been observed across the electromagnetic spectrum, from beyond 10 TeV by LHAASO [18, 19] down to radio frequencies [17].

3. H.E.S.S. Observations and Analysis

The High Energy Stereoscopic System (H.E.S.S.) is a system of five Imaging Atmospheric Telescopes located in the Khomas Highland of Namibia (23°16′18″, 16°30′00″) at 1800 m above sea level. Four 12-m telescopes (CT1-4) [20], each with a mirror area of 108 m^2, are placed in a square formation with 120 m side. A fifth, 28-m telescope (CT5) with a mirror area of 612 m^2 is placed in the center of the array [21], but it is not used in this contribution.

Observations of GRBs by HESS are facilitated through an automated alert system, which operates during observation time for prompt observations and is manually scheduled when the burst is not immediately visible for afterglow observations. GRB alerts are primarily transmitted by various space and ground-based facilities via the General Coordinates Network (GCN) [22]. The GCN disseminates these alerts, containing detailed information about the GRB triggers, to other experiments such as H.E.S.S to facilitate rapid follow-up observations. Within H.E.S.S's GRB

observation program, alerts from the Neil Gehrels Swift Observatory and the *Fermi* Gamma-ray Space Telescope undergo a filtering process. It's worth noting that H.E.S.S also receives alerts related to other transients like neutrinos and gravitational waves, which correspond to a distinct science program.

On October 9th, 2022, at 13:16:59 UTC, GRB 221009A was detected and localized by the Fermi Gamma-ray Burst Monitor, followed by the Neil Gehrels Swift Burst Alert Telescope. H.E.S.S., however, was unable to observe the burst immediately due to the presence of the full moon, which resulted in a high night sky background that prevented the operation of the highly sensitive instruments. Nevertheless, observations became feasible two days later, on October 11th, approximately T_0+51 hours after the initial detection, and continued for over a week. Unfortunately, the observational campaign was significantly affected by unfavorable atmospheric conditions, including cloudy skies and a high level of aerosol content.

On the third night following the trigger, H.E.S.S. conducted an extended 32-minute observation run under nominal conditions during dark time. This was followed by a second run using settings optimized for observations in the presence of high levels of optical background light, such as moonlight [23]. The total exposure time for H.E.S.S. observations amounted to nearly 5.6 hours. The zenith angle ranged from 47 degrees to 67 degrees, with the energy threshold increasing accordingly.

Throughout the observations, the atmospheric conditions remained poor, even on the subsequent nights, due to the presence of clouds and a higher concentration of aerosols in the atmosphere resulting from regular biomass burning activities [24]. The quality of atmospheric conditions is assessed using the atmospheric transparency coefficient [25], where lower values correspond to a reduced transmission of Cherenkov light through the atmosphere. Ideally, the atmospheric transparency coefficient should be above 0.8. However, during the H.E.S.S. observations of this GRB, the transparency coefficients were lower, necessitating a correction procedure [26]. Additional datasets taken on other nights were excluded from the analysis due to further degradation of atmospheric conditions caused by cloud cover.

The analysis of the data was carried out utilizing the ImPACT reconstruction procedure, as detailed in [27]. This procedure incorporates an independent event calibration and reconstruction methodology. The background estimation was performed using standard techniques outlined in [28].

To ensure the robustness of the results, a second, independent analysis was conducted using the method described in [29, 30], which employs standard gamma-hadron separation techniques and event selection criteria. The outcomes obtained from this secondary analysis served as a validation of the primary analysis.

There is no significant VHE gamma rays emission at the GRB location in the combined dataset nor for each night separately. The calculation of the flux upper limit is carried out using the Rolke method, assuming a power-law spectrum with a photon index of 2 [31]. The minimum energy sets the lower limit of the spectral analysis and is defined as the lowest energy at which the bias between reconstructed and simulated energies is below 10%. The maximum energy is chosen in a way that ensures the number of background events $N_{\mathrm{OFF}} \geq 10$. For each night, we calculate integral flux upper limits in the energy range [Ethr, 10] TeV. Since gamma-rays with energies above a few hundred GeV are strongly attenuated by the Extragalactic Background Light (EBL), we used [32] model to correct the attenuation. The H.E.S.S.integrated energy flux limits are shown in Figure 2.

4. Multiwavelength observations

We conducted X-ray analysis in the energy range of approximately 0.3-10 keV using data from the X-Ray Telescope (XRT) on the Neil Gehrels Swift Observatory [33, 34]. The analysis was performed using the HEASOFT software [35]. The time intervals are selected to align with the H.E.S.S. observations, ensuring overlap between the two. Since there were no simultaneous XRT observations during two out of the three H.E.S.S. nights, we define the time ranges to encompass a single continuous set of XRT observations before and after the H.E.S.S. observations. However, for the first night of H.E.S.S. observations, following this rule resulted in a lower XRT exposure time than desired. Therefore, for this particular night, we extend the time range to include two sets of continuous XRT observations on both sides to ensure an adequate exposure time.

5. Results

No evidence of VHE gamma-ray detection was found at the location of the GRB in both the combined dataset and when analyzing each night separately as shown in Figure 1.

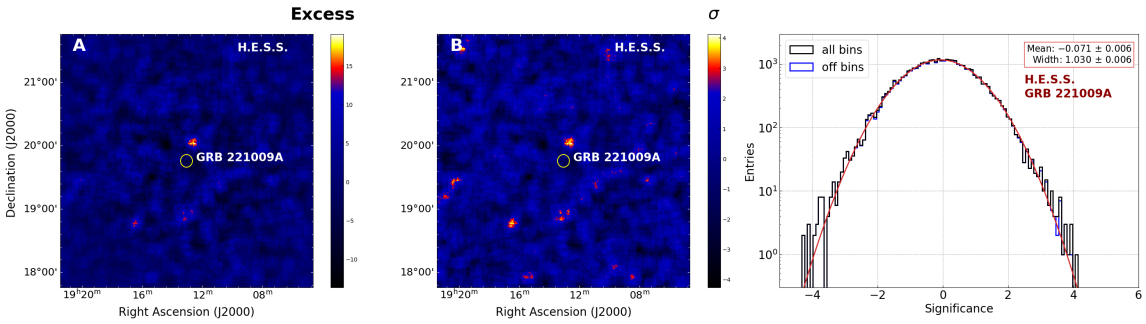

Figure 1: From left to right, the Excess count map with a 0.1° oversampling radius (yellow circle), the Significance map computed from the H.E.S.S. excess count map and the 1-D Significance distribution of the H.E.S.S. significance map entries in black and a Gaussian distribution fit in red. For details see [8]

We produced a multi-wavelength Spectral Energy Distribution (SED) from radio to VHE bands for the third night after the trigger. An example set of synchrotron and SSC emission components — arising from a single, partially cooled electron population is also presented. For details and text see [8].

Finally, we produced a multiwavelength light curve comparing the Swift-XRT and the entire H.E.S.S observation period. We then added a step further and put the H.E.S.S. limits into LHASSO[19] context by extrapolating their slow decaying exponential cutoff broken power law to the H.E.S.S. observation energy range. The light curve is presented in Figure 2, see also [8] for details.

6. Discussion and Conclusions

We presented the H.E.S.S. follow-up observation of the GRB 221009A after 51.6 hours since the trigger. While no significant VHE gamma-ray excess was detected in the study of the GRB,

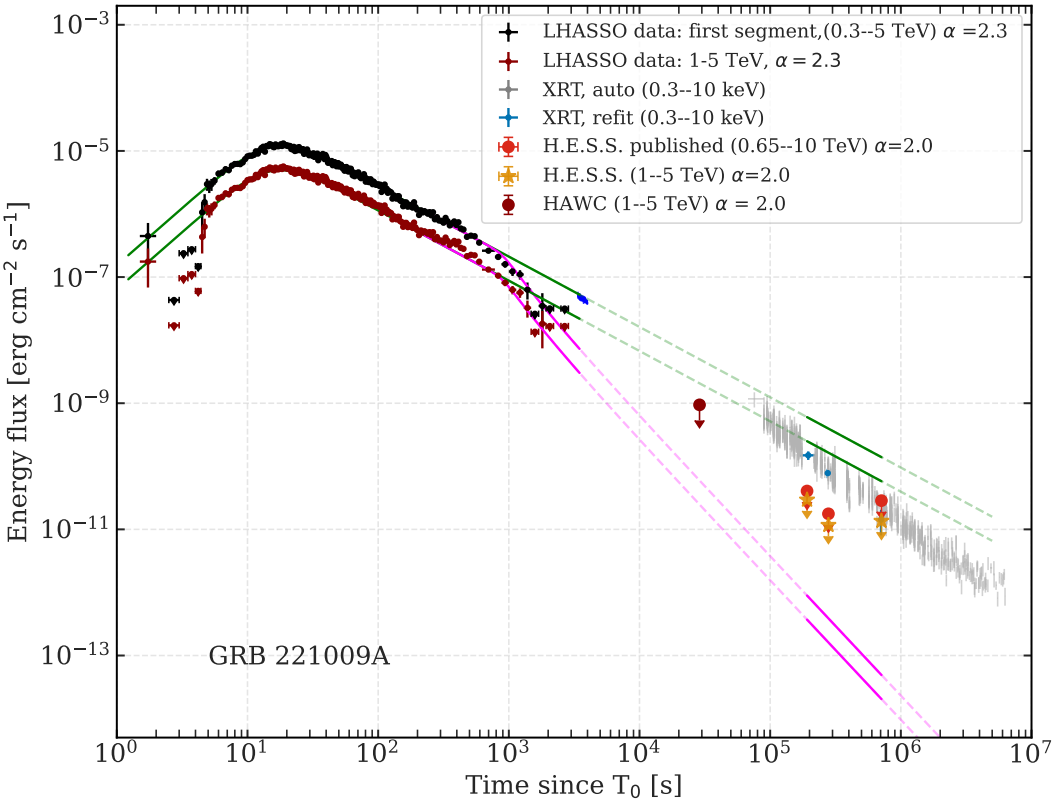

Figure 2: The H.E.S.S. integral energy flux upper limits (red circles; 95% C.L.) are derived assuming an intrinsic E^{-2} spectrum [8]. The LHASSO energy fluxes integrated within 1–5 TeV energy range are shown for comparison to HAWC and HESS in the same energy range.

the limits derived contributed valuable insights into modeling and demonstrated the importance of multi-messenger observations in understanding Very high-energy astrophysical phenomena. The light curve shows that we are constraining the LHASSO observations, especially their slow decay function, which has a temporal spectral index of $\alpha = -1.115 \pm 0.012$. The steep decay function has a temporal spectral index of $\alpha = -2.21^{+0.30}_{-0.83}$. The synchrotron + SSC emission components arising from a single, partially cooled electron population was considered to illustrate a possible explanation of the multiwavelength observations including H.E.S.S..

References

[1] T. Piran *Physics Reports* **314** no. 6, (1999) 575–667.

[2] S. Woosley and J. Bloom *Annual Review of Astronomy and Astrophysics* **44** no. 1, (2006) 507–556.

[3] E. Berger *Annual Review of Astronomy and Astrophysics* **52** no. 1, (2014) 43–105.

[4] B. P. Abbott, R. Abbott, and Abbott et al. *APJL* **848** no. 2, (Oct., 2017) L12.

[5] B. D. Metzger *Living Reviews in Relativity* **20** no. 1, (May, 2017) 3.

[6] Abdalla et al. (H.E.S.S. Collaboration) *Science* **372** no. 6546, (June, 2021) 1081–1085.

[7] MAGIC Collaboration **575** no. 7783, (Nov., 2019) 455–458.

[8] F. Aharonian et al. (H.E.S.S. Collaboration) *The Astrophysical Journal Letters* **946** no. 1, (Mar, 2023) L27.

[9] P. Veres, E. Burns, E. Bissaldi, S. Lesage, O. Roberts, and Fermi GBM Team *GRB Coordinates Network* **32636** (Oct., 2022) 1.

[10] E. Bissaldi, N. Omodei, M. Kerr, and Fermi-LAT Team *GRB Coordinates Network* **32637** (Oct., 2022) 1.

[11] S. Dichiara, J. D. Gropp, J. A. Kennea, N. P. M. Kuin, A. Y. Lien, F. E. Marshall, A. Tohuvavohu, M. A. Williams, and Neil Gehrels Swift Observatory Team *GRB Coordinates Network* **32632** (Oct., 2022) 1.

[12] E. B. et. al. *The Astrophysical Journal Letters* **946** no. 1, (Mar, 2023) L31.

[13] A. de Ugarte Postigo, L. Izzo, G. Pugliese, D. Xu, B. Schneider, J. P. U. Fynbo, N. R. Tanvir, D. B. Malesani, A. Saccardi, D. A. Kann, K. Wiersema, B. P. Gompertz, C. C. Thoene, A. J. Levan, and Stargate Collaboration *GRB Coordinates Network* **32648** (Oct., 2022) 1.

[14] Malesani et al. *arXiv e-prints* (Feb., 2023) arXiv:2302.07891.

[15] D. Frederiks, D. Svinkin, A. L. Lysenko, S. Molkov, A. Tsvetkova, M. Ulanov, A. Ridnaia, A. A. Lutovinov, I. Lapshov, A. Tkachenko, and V. Levin *The Astrophysical Journal Letters* **949** no. 1, (May, 2023) L7.

[16] Lesage et al. *arXiv e-prints* (Mar., 2023) arXiv:2303.14172.

[17] M. D. Fulton, S. J. Smartt, Rhodes, *et al.*, "The optical light curve of grb 221009a: the afterglow and detection of the emerging supernova sn 2022xiw," 2023. https://arxiv.org/abs/2301.11170.

[18] Y. Huang, S. Hu, S. Chen, M. Zha, C. Liu, Z. Yao, Z. Cao, and T. L. Experiment *GRB Coordinates Network* **32677** (Oct., 2022) 1.

[19] **LHASSO** Collaboration, Z. Cao *et al. Science* **0** no. 0, (June, 2023) eadg9328.

[20] Aharonian, F. *et al. A&A* **457** no. 3, (2006) 899–915.

[21] **H.E.S.S.** Collaboration, M. Holler *et al. PoS* **ICRC2015** (2015) 847.

[22] S. Barthelmy, E. Burns, D. Dutko, M. Gibb, V. Gonzalez-Leon, T. Jaffe, R. Lorek, I. Martinez, T. McGlynn, J. Racusin, D. Simpson, L. Singer, T. Sheets, A. Smale, D. Tak, Gcn, Tach, and Heasarc *GRB Coordinates Network* **32419** (July, 2022) 1.

[23] L. Tomankova, A. Yusafzai, D. Kostunin, G. Giavitto, S. Ohm, A. Mitchell, M. de Naurois, J.-P. Lenain, and H. Collaboration *Zenodo* **https://doi.org/10.5281/zenodo.7400326** (Dec., 2022) .

[24] P. Formenti, B. D'Anna, C. Flamant, *et al.* *Bulletin of the American Meteorological Society* **100** no. 7, (2019) 1277 – 1298.

[25] J. Hahn, R. de los Reyes, K. Bernlöhr, P. Krüger, Y. Lo, P. Chadwick, M. Daniel, C. Deil, H. Gast, K. Kosack, and V. Marandon *Astroparticle Physics* **54** (2014) 25–32.

[26] T. L. Holch, F. Leuschner, J. Schäfer, and S. Steinmassl *Journal of Physics: Conference Series* **2398** no. 1, (Dec, 2022) 012017.

[27] R. D. Parsons and J. A. Hinton *Astroparticle Physics* **56** (Apr., 2014) 26–34.

[28] D. Berge, Funk, S., and Hinton, J. *A&A* **466** no. 3, (2007) 1219–1229.

[29] M. de Naurois and L. Rolland *Astroparticle Physics* **32** no. 5, (2009) 231–252.

[30] M. Holler *et al.* *Astroparticle Physics* **123** (2020) 102491.

[31] W. A. Rolke, A. M. López, and J. Conrad *NIM-A* **551** no. 2, (2005) 493–503.

[32] A. Domínguez, J. R. Primack, D. J. Rosario, F. Prada, R. C. Gilmore, S. M. Faber, D. C. Koo, R. S. Somerville, M. A. Pérez-Torres, P. Pérez-González, J.-S. Huang, M. Davis, P. Guhathakurta, P. Barmby, C. J. Conselice, M. Lozano, J. A. Newman, and M. C. Cooper **410** (Feb., 2011) 2556–2578.

[33] N. Gehrels *et al.* *ApJ* **611** (Aug., 2004) 1005–1020.

[34] D. N. Burrows *et al.* *SSR* **120** (Oct., 2005) 165–195.

[35] P. A. Evans *et al.* *MNRAS* **397** no. 3, (07, 2009) 1177–1201.

F. Aharonian[1,2,3], F. Ait Benkhali[4], A. Alkan[5], J. Aschersleben[6], H. Ashkar[7], M. Backes[8,9], A. Baktash[10], V. Barbosa Martins[11], A. Barnacka[12], J. Barnard[13], R. Batzofin[14], Y. Becherini[15,16], G. Beck[17], D. Berge[11,18], K. Bernlöhr[2], B. Bi[19], M. Böttcher[9], C. Boisson[20], J. Bolmont[21], M. de Bony de Lavergne[5], J. Borowska[18], M. Bouyahiaoui[2], F. Bradascio[5], M. Breuhaus[2], R. Brose[1], A. Brown[22], F. Brun[5], B. Bruno[23], T. Bulik[24], C. Burger-Scheidlin[1], T. Bylund[5], F. Cangemi[21], S. Caroff[25], S. Casanova[26], R. Cecil[10], J. Celic[23], M. Cerruti[15], P. Chambery[27], T. Chand[9], S. Chandra[9], A. Chen[17], J. Chibueze[9], O. Chibueze[9], T. Collins[28], G. Cotter[22], P. Cristofari[20], J. Damascene Mbarubucyeye[11], I.D. Davids[8], J. Davies[22], L. de Jonge[9], J. Devin[29], A. Djannati-Ataï[15], J. Djuvsland[2], A. Dmytriiev[9], V. Doroshenko[19], L. Dreyer[9], L. Du Plessis[9], K. Egberts[14], S. Einecke[28], J.-P. Ernenwein[30], S. Fegan[7], K. Feijen[15], G. Fichet de Clairfontaine[20], G. Fontaine[7], F. Lott[8], M. Füßling[11], S. Funk[23], S. Gabici[15], Y.A. Gallant[29], S. Ghafourizadeh[4], G. Giavitto[11], L. Giunti[15,5], D. Glawion[23], J.F. Glicenstein[5], J. Glombitza[23], P. Goswami[15], G. Grolleron[21], M.-H. Grondin[27], L. Haerer[2], S. Hattingh[9], M. Haupt[11], G. Hermann[2], J.A. Hinton[2], W. Hofmann[2], T. L. Holch[11], M. Holler[31], D. Horns[10], Zhiqiu Huang[2], A. Jaitly[11], M. Jamrozy[12], F. Jankowsky[4], A. Jardin-Blicq[27], V. Joshi[23], I. Jung-Richardt[23], E. Kasai[8], K. Katarzyński[32], H. Katjaita[8], D. Khangulyan[33], R. Khatoon[9], B. Khélifi[15], S. Klepser[11], W. Kluźniak[34], Nu. Komin[17], R. Konno[11], K. Kosack[5], D. Kostunin[11], A. Kundu[9], G. Lamanna[25], R.G. Lang[23], S. Le Stum[30], V. Lefranc[5], F. Leitl[23], A. Lemière[15], M. Lemoine-Goumard[27], J.-P. Lenain[21], F. Leuschner[19], A. Luashvili[20], I. Lypova[4], J. Mackey[1], D. Malyshev[19], D. Malyshev[23], V. Marandon[5], A. Marcowith[29], P. Marinos[28], G. Martí-Devesa[31], R. Marx[4], G. Maurin[25], A. Mehta[11], P.J. Meintjes[13], M. Meyer[10], A. Mitchell[23], R. Moderski[34], L. Mohrmann[2], A. Montanari[4], C. Moore[35], E. Moulin[5], T. Murach[11], K. Nakashima[23], M. de Naurois[7], H. Ndiyavala[8,9], J. Niemiec[26], A. Priyana Noel[12], P. O'Brien[35], S. Ohm[11], L. Olivera-Nieto[2], E. de Ona Wilhelmi[11], M. Ostrowski[12], E. Oukacha[15], S. Panny[31], M. Panter[2], R.D. Parsons[18], U. Pensec[21], G. Peron[15], S. Pita[15], V. Poireau[25], D.A. Prokhorov[36], H. Prokoph[11], G. Pühlhofer[19], M. Punch[15], A. Quirrenbach[4], M. Regeard[15], P. Reichherzer[5], A. Reimer[31], O. Reimer[31], I. Reis[5], Q. Remy[2], H. Ren[2], M. Renaud[29], B. Reville[2], F. Rieger[2], G. Roellinghoff[23], E. Rol[36], G. Rowell[28], B. Rudak[34], H. Rueda Ricarte[5], E. Ruiz-Velasco[2], K. Sabri[29], V. Sahakian[37], S. Sailer[2], H. Salzmann[19], D.A. Sanchez[25], A. Santangelo[19], M. Sasaki[23], J. Schäfer[23], F. Schüssler[5], H.M. Schutte[9], M. Senniappan[16], J.N.S. Shapopi[8], S. Shilunga[8], K. Shiningayamwe[8], H. Sol[20], H. Spackman[22], A. Specovius[23], S. Spencer[23], Ł. Stawarz[12], R. Steenkamp[8], C. Stegmann[14,11], S. Steinmassl[2], C. Steppa[14], K. Streil[23], I. Sushch[9], H. Suzuki[38], T. Takahashi[39], T. Tanaka[38], T. Tavernier[5], A.M. Taylor[11], R. Terrier[15], A. Thakur[28], J. H.E. Thiersen[9], C. Thorpe-Morgan[19], M. Tluczykont[10], M. Tsirou[11], N. Tsuji[40], R. Tuffs[2], Y. Uchiyama[33], M. Ullmo[5], T. Unbehaun[23], P. van der Merwe[9], C. van Eldik[23], B. van Soelen[13], G. Vasileiadis[29], M. Vecchi[6], J. Veh[23], C. Venter[9], J. Vink[36], H.J. Völk[2], N. Vogel[23], T. Wach[23], S.J. Wagner[4], F. Werner[2], R. White[2], A. Wierzcholska[26], Yu Wun Wong[23], H. Yassin[9], M. Zacharias[4,9], D. Zargaryan[1], A.A. Zdziarski[34], A. Zech[20], S.J. Zhu[11], A. Zmija[23], S. Zouari[15] and N. Żywucka[9].

[1]Dublin Institute for Advanced Studies, 31 Fitzwilliam Place, Dublin 2, Ireland
[2]Max-Planck-Institut für Kernphysik, P.O. Box 103980, D 69029 Heidelberg, Germany
[3]Yerevan State University, 1 Alek Manukyan St, Yerevan 0025, Armenia
[4]Landessternwarte, Universität Heidelberg, Königstuhl, D 69117 Heidelberg, Germany
[5]IRFU, CEA, Université Paris-Saclay, F-91191 Gif-sur-Yvette, France
[6]Kapteyn Astronomical Institute, University of Groningen, Landleven 12, 9747 AD Groningen, The Netherlands
[7]Laboratoire Leprince-Ringuet, École Polytechnique, CNRS, Institut Polytechnique de Paris, F-91128 Palaiseau, France
[8]University of Namibia, Department of Physics, Private Bag 13301, Windhoek 10005, Namibia
[9]Centre for Space Research, North-West University, Potchefstroom 2520, South Africa
[10]Universität Hamburg, Institut für Experimentalphysik, Luruper Chaussee 149, D 22761 Hamburg, Germany
[11]Deutsches Elektronen-Synchrotron DESY, Platanenallee 6, 15738 Zeuthen, Germany
[12]Obserwatorium Astronomiczne, Uniwersytet Jagielloński, ul. Orla 171, 30-244 Kraków, Poland
[13]Department of Physics, University of the Free State, PO Box 339, Bloemfontein 9300, South Africa
[14]Institut für Physik und Astronomie, Universität Potsdam, Karl-Liebknecht-Strasse 24/25, D 14476 Potsdam, Germany
[15]Université de Paris, CNRS, Astroparticule et Cosmologie, F-75013 Paris, France
[16]Department of Physics and Electrical Engineering, Linnaeus University, 351 95 Växjö, Sweden
[17]School of Physics, University of the Witwatersrand, 1 Jan Smuts Avenue, Braamfontein, Johannesburg, 2050 South Africa
[18]Institut für Physik, Humboldt-Universität zu Berlin, Newtonstr. 15, D 12489 Berlin, Germany
[19]Institut für Astronomie und Astrophysik, Universität Tübingen, Sand 1, D 72076 Tübingen, Germany
[20]Laboratoire Univers et Théories, Observatoire de Paris, Université PSL, CNRS, Université Paris Cité, 5 Pl. Jules Janssen, 92190 Meudon, France
[21]Sorbonne Université, Université Paris Diderot, Sorbonne Paris Cité, CNRS/IN2P3, Laboratoire de Physique Nucléaire et de Hautes Energies, LPNHE, 4 Place Jussieu, F-75252 Paris, France
[22]University of Oxford, Department of Physics, Denys Wilkinson Building, Keble Road, Oxford OX1 3RH, UK
[23]Friedrich-Alexander-Universität Erlangen-Nürnberg, Erlangen Centre for Astroparticle Physics, Nikolaus-Fiebiger-Str. 2, 91058 Erlangen, Germany
[24]Astronomical Observatory, The University of Warsaw, Al. Ujazdowskie 4, 00-478 Warsaw, Poland
[25]Université Savoie Mont Blanc, CNRS, Laboratoire d'Annecy de Physique des Particules - IN2P3, 74000 Annecy, France
[26]Instytut Fizyki Jądrowej PAN, ul. Radzikowskiego 152, 31-342 Kraków, Poland
[27]Université Bordeaux, CNRS, LP2I Bordeaux, UMR 5797, F-33170 Gradignan, France
[28]School of Physical Sciences, University of Adelaide, Adelaide 5005, Australia
[29]Laboratoire Univers et Particules de Montpellier, Université Montpellier, CNRS/IN2P3, CC 72, Place Eugène Bataillon, F-34095

PoS(ICRC2023)705

Montpellier Cedex 5, France
[30]Aix Marseille Université, CNRS/IN2P3, CPPM, Marseille, France
[31]Universität Innsbruck, Institut für Astro- und Teilchenphysik, Technikerstraße 25, 6020 Innsbruck, Austria
[32]Institute of Astronomy, Faculty of Physics, Astronomy and Informatics, Nicolaus Copernicus University, Grudziadzka 5, 87-100 Torun, Poland
[33]Department of Physics, Rikkyo University, 3-34-1 Nishi-Ikebukuro, Toshima-ku, Tokyo 171-8501, Japan
[34]Nicolaus Copernicus Astronomical Center, Polish Academy of Sciences, ul. Bartycka 18, 00-716 Warsaw, Poland
[35]Department of Physics and Astronomy, The University of Leicester, University Road, Leicester, LE1 7RH, United Kingdom
[36]GRAPPA, Anton Pannekoek Institute for Astronomy, University of Amsterdam, Science Park 904, 1098 XH Amsterdam, The Netherlands
[37]Yerevan Physics Institute, 2 Alikhanian Brothers St., 0036 Yerevan, Armenia
[38]Department of Physics, Konan University, 8-9-1 Okamoto, Higashinada, Kobe, Hyogo 658-8501, Japan
[39]Kavli Institute for the Physics and Mathematics of the Universe (WPI), The University of Tokyo Institutes for Advanced Study (UTIAS), The University of Tokyo, 5-1-5 Kashiwa-no-Ha, Kashiwa, Chiba, 277-8583, Japan
[40]RIKEN, 2-1 Hirosawa, Wako, Saitama 351-0198, Japan

PoS(ICRC2023)705